

RUTHENIUM(III) ACETYLACETONATE AS CATALYST PRECURSOR
IN THE DEHYDROGENATION OF
DIMETHYLAMINE-BORANE

A THESIS SUBMITTED TO
THE GRADUATE SCHOOL OF NATURAL AND APPLIED SCIENCES
OF
MIDDLE EAST TECHNICAL UNIVERSITY

BY

EBRU ÜNEL

IN PARTIAL FULFILLMENT OF THE REQUIREMENTS
FOR
THE DEGREE OF MASTER OF SCIENCE
IN
CHEMISTRY

FEBRUARY 2011

Approval of the thesis:

**RUTHENIUM(III) ACETYLACETONATE AS CATALYST
PRECURSOR IN THE DEHYDROGENATION OF
DIMETHYLAMINE-BORANE**

submitted by **EBRU ÜNEL** in partial fulfillment of the requirements for the degree of **Master of Science in Chemistry Department, Middle East Technical University** by,

Prof. Dr. Canan Özgen

Dean, Graduate School of **Natural and Applied Sciences**

Prof. Dr. İlker Özkan

Head of Department, **Chemistry**

Prof. Dr. Saim Özkar

Supervisor, **Chemistry Department, METU**

Examining Committee Members:

Prof. Dr. Ceyhan Kayran

Chemistry Dept., METU

Prof. Dr. Saim Özkar

Chemistry Dept., METU

Prof. Dr. Birgül Karan

Chemistry Dept., Hacettepe University

Assoc. Prof. Dr. Ayşen Yılmaz

Chemistry Dept., METU

Assist. Prof. Dr. Emren Esentürk

Chemistry Dept., METU

Date: February 2011

I hereby declare that all information in this document has been obtained and presented in accordance with academic rules and ethical conduct. I also declare that, as required by these rules and conduct, I have fully cited and referenced all materials and results that are not original to this work.

Name, Last name: Ebru Ünel

Signature:

ABSTRACT

RUTHENIUM(III) ACETYLACETONATE AS CATALYST PRECURSOR IN THE DEHYDROGENATION OF DIMETHYLAMINE-BORANE

Ünel, Ebru

M. Sc., Department of Chemistry

Supervisor: Prof. Dr. Saim Özkar

February 2011, 40 pages

Amine boranes have recently been considered as solid hydrogen storage materials with high capability of hydrogen storage. Dimethylamine borane is one of the promising amine boranes with high theoretical gravimetric capacity of 16.9 wt%. Dimethylamine borane can undergo dehydrogenation only in the presence of a suitable catalyst at moderate temperature.

In this project, throughout the dehydrogenation of dimethylamine borane (DMAB), the catalytic activity of ruthenium(III) acetylacetonate was examined for the first time. During the catalytic reaction, formation of a new in-situ ruthenium(II) species, $[\text{Ru}\{\text{N}_2\text{Me}_4\}_3(\text{acac})\text{H}]$, is observed. Mercury poisoning experiment indicates that the in-situ ruthenium(II) species is a homogeneous catalyst in the dehydrogenation of dimethylamine borane. Kinetics of catalytic dehydrogenation of dimethylamine borane starting with ruthenium(III) acetylacetonate was

investigated depending on catalyst concentration, substrate concentration and temperature. As a result, the hydrogen generation rate was found to be first-order with respect to catalyst concentration and zero-order regarding the substrate concentration. Besides, evaluation of the kinetic data yielded that the activation parameters for dehydrogenation reaction: the activation energy, $E_a = 85 \pm 2 \text{ kJ}\cdot\text{mol}^{-1}$; the enthalpy of activation, $\Delta H^\ddagger = 82 \pm 2 \text{ kJ}\cdot\text{mol}^{-1}$ and the entropy of activation; $\Delta S^\ddagger = -85 \pm 5 \text{ J}\cdot\text{mol}^{-1}\cdot\text{K}^{-1}$. Additionally, before deactivation, $[\text{Ru}\{\text{N}_2\text{Me}_4\}_3(\text{acac})\text{H}]$ provides 1700 turnovers over 100 hours in hydrogen evolution from the dehydrogenation of dimethylamine borane. $[\text{Ru}\{\text{N}_2\text{Me}_4\}_3(\text{acac})\text{H}]$ complex formed during the dehydrogenation of dimethylamine borane was isolated and characterized by UV-Visible, FTIR, ^1H NMR, and Mass Spectroscopy. The isolated ruthenium(II) species was also tested as homogeneous catalyst in the dehydrogenation of dimethylamine borane.

Keywords: Ruthenium; Acetylacetonate; Tetramethyl Hydrazine; Dimethylamine borane; Dehydrogenation; Homogeneous catalysis.

ÖZ

DİMETİLAMİN BORANIN DEHİDROJENLENMESİNDE KATALİZÖR BAŞLATICISI OLARAK RUTENYUM(III) ASETİLASETONAT

Ünel, Ebru

Yüksek Lisans, Kimya Bölümü

Tez Yöneticisi: Prof. Dr. Saim Özkar

Şubat 2011, 40 sayfa

Son zamanlarda, amin boranlar yüksek oranda hidrojen depolama yetenekleriyle, hidrojen depolayan katı materyaller olarak anılmaktadır. Dimetilamin boran ağırlıkça yüzde 16.9 hidrojen depolama kapasitesiyle amin boranların içinde gelecek vaat etmektedir. Dimetilamin boran mutedil sıcaklıklarda uygun bir katalizör varlığında dehidrojenasyona girebilir.

Bu projede, dimetilamin boranın dehidrojenlenme tepkimesinde rutenyum(III) asetilasetonatın katalitik aktivitesi incelendi. Katalitik tepkime süresince, yeni bir aktif rutenyum(II) bileşiği oluşmaktadır. Cıva zehirlenme deneyi, oluşan rutenyum(II) bileşiğinin dimetilamin boranın dehidrojenleme tepkimesinde homojen katalizör olduğunu göstermektedir. Katalizör derişimine, tepken derişimine ve sıcaklığa bağlı olarak, rutenyum(III) asetilasetonatla katalizlenmiş dimetilamin boranın dehidrojenlenme tepkimesinin kinetiği çalışıldı. Tepkime derecesinin,

katalizör derişimine göre birinci, tepken derişimine göre sıfırncı dereceden olduđu saptandı. Tepkime kinetiğinin deęerlendirilmesi sonucunda aktivasyon parametreleri: aktivasyon enerjisi; $E_a = 85 \pm 2 \text{ kJmol}^{-1}$, aktivasyon entalpisi; $\Delta H^\ddagger = 82 \pm 2 \text{ kJmol}^{-1}$ ve aktivasyon entropisi; $\Delta S^\ddagger = -85 \pm 5 \text{ Jmol}^{-1}\text{K}^{-1}$ olarak bulundu.

Oluşan rutenyum(II) bileşii dimetilamin boranın dehidrojenlenmesinde yüz saatin üzerinde toplam 1700 mol H_2 / mol Ru çevrim sayısı sağlamaktadır. Dimetilamin boranın dehidrojenlenme tepkimesi sonucunda $[\text{Ru}\{\text{N}_2\text{Me}_4\}_3(\text{acac})\text{H}]$ bileşii izole edilerek, UV-Vis, FTIR, $^1\text{H-NMR}$, ve Kütle Spektroskopisi teknikleri kullanılarak tanımlandı. İzole edilen $[\text{Ru}\{\text{N}_2\text{Me}_4\}_3(\text{acac})\text{H}]$ dimetilamin boranın dehidrojenlenmesinde homojen katalizör olarak test edilmiştir.

Anahtar Kelimeler: Rutenyum; Asetilasetonat; Tetrametil Hidrazin; Dimetilamin boran; Dehidrojenlenme; Homojen katalizör.

To my family...

ACKNOWLEDGEMENTS

I would like to express my deep and sincere gratitude to my advisor Prof. Dr. Saim Özkar. His wide knowledge and his logical way of thinking have been of great value for me. His understanding, encouraging and personal guidance have provided a good basis for the present thesis.

I gratefully thank to Mehdi Masjedi for his support, valuable ideas and motivation during my studies.

I wish to express my sincere appreciation to Mehmet Zahmakıran for his support, answering my never ending questions and guidance to improve my skills during my study.

I owe many thanks to my lab partners Huriye Erdoğan, Serdar Akbayrak, Tuğçe Ayvalı, Salim Çalışkan who always ready to give a hand whenever I needed.

I truly thank to my dearest friends Zafer Öztürk, Berrin Özkan, Meryem Karabulut, Tuğba Orhan, Feriye Şenol who were with me in this challenging process for their precious friendship.

The last but not least, I would like to extend my gratitude to my parents Ahmet Ünel, Günnur Ünel and my twin sister Burcu Ünel, for helping me with every problem I encountered during the whole study and being next to me whenever I need.

TABLE OF CONTENTS

ABSTRACT	iv
ÖZ	vi
ACKNOWLEDGEMENTS	ix
TABLE OF CONTENTS.....	x
LIST OF TABLES	xii
LIST OF FIGURES	xiii
CHAPTERS	
1.INTRODUCTION	1
2. EXPERIMENTAL.....	7
2.1. Materials	7
2.2. Equipment.....	7
2.3. Catalytic dehydrogenation of dimethylamine borane by using ruthenium(III) acetylacetonate.....	9
2.4. Catalytic lifetime of ruthenium(III) acetylacetonate pre-catalyst .	10
2.5. Poisoning experiment.....	10
2.6. Isolation and characterization of in-situ ruthenium(II) species, [Ru{N ₂ Me ₄ } ₃ (acac)H].....	11
3. RESULTS AND DISCUSSION	12
3.1. Catalytic dehydrogenation of dimethylamine borane starting with Ru(acac) ₃	12

3.2. UV-Visible Spectra	15
3.3. Isolation of the ruthenium(II) species	17
3.3.1. Infrared Spectrum	18
3.3.2. Mass Spectrum	18
3.3.3. ¹ H-NMR Spectrum	19
3.3.4 The in-situ formation of ruthenium(II) species, [Ru{N ₂ Me ₄ } ₃ (acac)H], during the catalytic dehydrogenation of dimethylamine borane starting with Ru(acac) ₃	20
3.4. Poisoning Experiments.....	22
3.5. Activity of Isolated Ruthenium Species, [Ru{N ₂ Me ₄ } ₃ (acac)H].....	23
3.6. Kinetic Study.....	24
3.7 The Catalytic Life Time of Active Catalyst.....	33
4. CONCLUSIONS.....	35
REFERENCES.....	37

LIST OF TABLES

TABLES

Table 1.1 Dehydrogenation of Me_2NHBH_3 to yield $[\text{Me}_2\text{N-BH}_2]_2$ using various transition metal catalysts [43].	4
Tablo 3.1 Values of the rate constant k in $(\text{mol H}_2) \cdot (\text{mol Ru})^{-1} \cdot \text{s}^{-1}$ for dehydrogenation of dimethylamine borane (500 mM) catalyzed by ruthenium(III) acetylacetonate (5 mM) at different temperatures.	30

LIST OF FIGURES

FIGURES

Figure 1.1 Crystal structure of Ru(acac) ₃ acting as homogeneous catalyst in the dehydrogenation of dimethylamine borane.....	6
Figure 2.1 The Parr 5101 Low Pressure Stirred Reactor used in catalytic dehydrogenation of dimethylamine borane and measuring the generation of hydrogen from the reaction.....	8
Figure 3.1 ¹¹ B NMR spectra of the reaction medium before and after the reaction at 60 °C ([DMAB] = 500mM and [Ru] = 5mM).	13
Figure 3.2 Plots of hydrogen volume versus time for the dehydrogenation of dimethylamine borane (500 mM) catalyzed by Ru(acac) ₃ (5mM) as pre-catalyst at different temperatures.	14
Figure 3.3 Plots of hydrogen volume versus time for the dehydrogenation of dimethylamine borane (500 mM) catalyzed by Ru(acac) ₃ (5mM) as pre-catalyst in 10 mL toluene at 60 °C.	15
Figure 3.4 UV-visible electronic absorption spectra recorded during the catalytic dehydrogenation of dimethylamine borane starting with Ru(acac) ₃	17
Figure 3.5 FTIR spectrum of the isolated ruthenium(II) species after catalytic dehydrogenation of dimethylamine borane (500mM) starting with Ru(acac) ₃ (5mM), taken from the ATR unit.....	18
Figure 3.6 Mass spectrum of the ruthenium species, [Ru{N ₂ Me ₄ } ₃ (acac)H], isolated after catalytic dehydrogenation of dimethylamine borane starting with Ru(acac) ₃	19

Figure 3.7 ^1H NMR spectrum of the ruthenium species, $[\text{Ru}\{\text{N}_2\text{Me}_4\}_3(\text{acac})\text{H}]$, isolated after catalytic dehydrogenation of dimethylamine borane (500 mM) starting with $\text{Ru}(\text{acac})_3$ (5mM).....	20
Figure 3.8 A new in situ ruthenium(II) species, $[\text{Ru}\{\text{N}_2\text{Me}_4\}_3(\text{acac})\text{H}]$	21
Figure 3.9 ^{11}B NMR spectrum of $\text{B}(\text{OMe})_3$	22
Figure 3.10 Comparison of dehydrogenation of dimethylamine borane (500 mM) catalyzed by $\text{Ru}(\text{acac})_3$ (5 mM) and isolated ruthenium species, $[\text{Ru}\{\text{N}_2\text{Me}_4\}_3(\text{acac})\text{H}]$ (1.65 mM) at 60.0 ± 0.1 °C. The data obtained for the latter complex was corrected by a factor of 3.	24
Figure 3.11 Plots of hydrogen volume versus time for the dehydrogenation of dimethylamine borane (500 mM) catalyzed by $\text{Ru}(\text{acac})_3$ as pre-catalyst with different ruthenium concentrations at 60°C.....	25
Figure 3.12 Plot of hydrogen generation rate versus the concentration of ruthenium (both in logarithmic scales) for the dehydrogenation of dimethylamine borane (500 mM) started with $\text{Ru}(\text{acac})_3$ at 60 °C after the induction time.....	26
Figure 3.13 Plots of hydrogen volume versus time for the dehydrogenation of dimethylamine borane catalyzed by 5 mM $\text{Ru}(\text{acac})_3$ as pre-catalyst with different substrate concentrations at 60°C.....	27
Figure 3.14 Plot of hydrogen generation rate versus the concentration of dimethylamine borane (both in logarithmic scales) for the dehydrogenation of dimethylamine borane started with $\text{Ru}(\text{acac})_3$ (5 mM) at 60 °C after the induction time.....	28
Figure 3.15 Plots of hydrogen volume versus time for dehydrogenation of dimethylamine borane starting with a solution containing 500 mM $\text{NH}(\text{CH}_3)_2\text{BH}_3$ and 5 mM $\text{Ru}(\text{acac})_3$ at various temperatures.....	29

Figure 3.16 Arrhenius plot for dehydrogenation of dimethylamine borane starting with a solution containing 500 mM $\text{NH}(\text{CH}_3)_2\text{BH}_3$ and 5 mM $\text{Ru}(\text{acac})_3$ at different temperatures.	31
Figure 3.17 Eyring plot for dehydrogenation of dimethylamine borane starting with a solution containing 500 mM $\text{NH}(\text{CH}_3)_2\text{BH}_3$ and 5 mM $\text{Ru}(\text{acac})_3$ at different temperatures.	32
Figure 3.18 Plot of total turnover number versus time for dehydrogenation of dimethylamine borane catalyzed by $\text{Ru}(\text{acac})_3$ pre-catalyst along with active catalyst at 60°C.	33

CHAPTER 1

INTRODUCTION

Fossil fuels are thought to be responsible for the today's most important environmental problem because of the carbon dioxide emission arising from the combustion of the fossil fuels since it constitutes 80% of the world energy demand [1]. Besides, since the fossil fuels are non-renewable energy sources and reserves of the fossil fuels decrease rapidly because of the increasing demand of energy, finding a renewable and environmentally friendly alternative solution is urgently needed [2]. Although, some source of energy like wind energy, solar energy, hydropower and biomass energy are clean and renewable, the non continuation of these sources and the high cost of these resources' power plants make these solutions inapplicable [3]. Therefore, in order to compensate day by day increase of energy needs, energy should be stored. At this point, hydrogen appears to be the best alternative energy carriers to move our energy economy from one based on fossil fuels to one based upon hydrogen since it is an efficient and clean energy supply [4].

Hydrogen storage materials such as metal hydrides [5], nanomaterials and metal organic frameworks [6] have been reported so far. However, there are still some challenges. The gravimetric and volumetric hydrogen capacities must be enhanced for hydrogen storage materials. Chemical hydrogen storage materials are expected as potential source of energy due

to their high hydrogen content. Among them, boron- and nitrogen-based compounds such as $\text{LiNH}_2\text{-LiH}$ and NaBH_4 have attracted a great deal of attention [7,8,9]. Besides, interest on amine boranes as candidates for hydrogen storage material is remarkable because of their hydrogen capacity, higher than that of gasoline [10], and the potential reversibility of hydrogen release reactions [11]. However, catalysts are needed to release hydrogen from amine borane compounds at efficient rates.

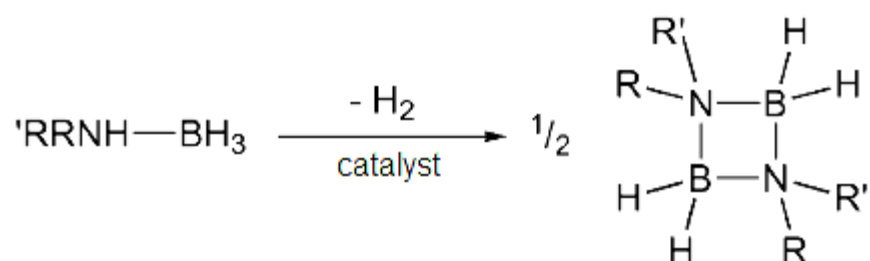
As solid materials, ammonia borane, NH_3BH_3 , and dimethylamine borane, $\text{NH}(\text{CH}_3)_2\text{BH}_3$, contain high theoretical gravimetric capacity of 19.6 wt % and 16.9 wt % of hydrogen, respectively. The Lewis acid BH_3 molecule can effectively act as a bifunctional catalyst for the H_2 elimination. This type of reaction is related to hydrolysis reactions in aqueous solution where the solvent water molecules undergo an active solvent catalysis facilitating the water addition by a relay of H-transfers [12]. Number of catalysts have been developed recently to improve the rate of H_2 elimination from amine borane and their methyl-substituted derivatives which are as follows: Rh catalysts including colloids, clusters, Rh(0) supported on alumina and oxide-supported metals [13,14,15,16,17,18,19,20]; Rh(0) and Cu(0) nanoclusters [21,22,23,24]; Ru(0) and Pd(0) nanoclusters [25]; Ru, Rh, Pd, Pt and Au nanoclusters supported on Al_2O_3 , C and SiO_2 [26]; Co, Ni and Cu supported on Al_2O_3 , C or SiO_2 [27]; doped platinum catalyst and K_2PtCl_6 salt [28,29]; $\text{Ni}_{1-x}\text{Pt}_x$ ($x = 0\text{-}0.12$) hollow spheres [30]; iridium and titanocene homogeneous catalysts [31,32]; Ni-NHC complexes (NHC = N-heterocyclic carbene) [33]; mesoporous silica materials [34]; cation exchange resins and zeolites as solid acids and carbon dioxide [35]; strong Lewis or Bronsted acids like tris(pentafluorophenyl)borane $\text{B}(\text{C}_6\text{F}_5)_3$ and trifluoromethane sulfonic acid (HOSO_2CF_3) [36] and ionic liquids [37]. In

addition to the hydrolysis and methanolysis, H₂ can be released from NH₃BH₃ through a pyrolysis route. Experimental and computational results have revealed that ammonia borane decomposes upon melting at 385 K with a hydrogen evolution of approximately 6.5 wt % of the initial mass, while the H₂ generation is moderately exothermic with a reaction enthalpy of -21 kJ·mol⁻¹ [38,39,40]. Another way of H₂ elimination from amine boranes is dehydrogenation. Primary and secondary amine borane adducts undergo dehydrogenation at elevated temperatures (>100 °C) to yield cyclic amine borane [R₂B-NR'₂]_x (x=2 or 3) and borazine [RB-NR']₃ derivatives. Among these amine boranes, dimethylamine borane undergoes thermally induced dehydrogenation at 130 °C in the melt to form the cyclic amineborane [Me₂N-BH₂]₂ [41]. The protic (H^{δ+}) and hydridic (H^{δ-}) hydrogen substituents at nitrogen and boron, respectively favors the hydrogen elimination from the intermolecular dehydrogenation Me₂NHBH₃. In order to carry out dehydrogenation process under mild conditions, a suitable catalyst is needed. As shown in Table 1.1 several catalysts were tested in dehydrogenation of Me₂NHBH₃ in toluene.

Table 1.1 Dehydrogenation of Me₂NHBH₃ in toluene to yield [Me₂N-BH₂]₂ using various transition metal catalysts [41].

Catalyst	T(°C)	Mol % catalyst	T(h)	Yield (%)
None	45		168	0
[Rh(1,5-cod)(μ-Cl)] ₂	25	0.5	8	100
[Rh(1,5-cod)(μ-Cl)] ₂	45	0.5	2	90
[Rh(1,5-cod)(μ-Cl)] ₂	25	5.0	<2	100
[Rh(1,5-cod)(μ-Cl)] ₂	45	5.0	<2	100
[Ir(1,5-cod)(μ-Cl)] ₂	25	0.5	136	95
RhCl ₃	25	0.5	22.5	90
RhCl ₃ .3H ₂ O	25	0.5	64	90
IrCl ₃	25	0.5	160	25
RhCl(PPh ₃) ₃	25	0.5	44	95
[Cp*Rh(μ-Cl)Cl] ₂	25	0.5	112	100
[Rh(1,5-cod) ₂]OTf	25	0.5	7.5	95
[Rh(1,5-cod)(dmpe)]PF ₆	25	0.5	112	95
HRh(CO)(PPh ₃) ₃	25	0.5	160	5
<i>trans</i> -RuMe ₂ (PMe ₃) ₄	25	0.5	16	100
<i>trans</i> -PdCl ₂ (P(<i>o</i> -tolyl) ₃) ₂	25	0.5	160	20
Pd/C (10%)	25	0.5	68	95
Cp ₂ TiMe ₂	25	0.5	160	0
B(C ₆ F ₅) ₃	25	0.5	96	0

No self dehydrogenation of dimethylamine borane is observed in the absence of a catalyst at 45 °C. The use of transition metal complexes as a catalyst in dehydrogenation of dimethylamine borane showed great variety in yield depending on temperature, reaction time and mol percentage of catalyst. Moreover, it is observed that while primary adducts or NH_3BH_3 afford borazine derivatives, secondary amine borane dehydrogenation pre-catalyzed by Rh, Ir, Ru and Pd results in monomeric and cyclodimeric aminoboranes [41].



In the hydrolysis of sodium borohydride, it is observed that ruthenium(III) acetylacetonate is acting as a homogeneous catalyst at room temperature providing 1200 turnovers over 3 h before its deactivation [42].

The observation that $\text{Ru}(\text{acac})_3$ acts as an effective homogeneous catalyst in the hydrolysis of NaBH_4 inspired us to test the catalytic activity of $\text{Ru}(\text{acac})_3$ in dehydrogenation of dimethylamine borane.

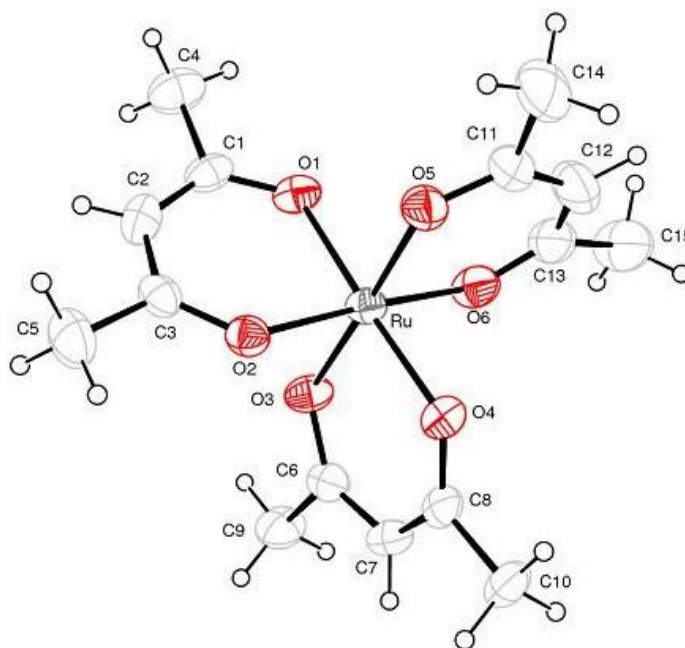
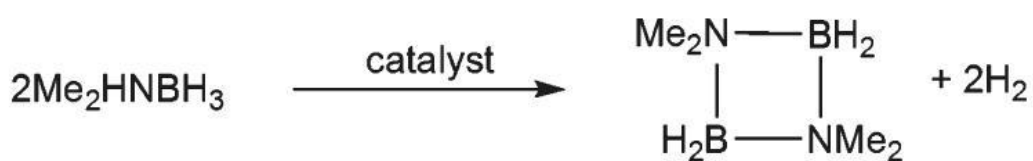


Figure 1.1 Crystal structure of $\text{Ru}(\text{acac})_3$ acting as homogeneous catalyst in the dehydrogenation of dimethylamine borane.

Altogether, the aim of this research is to investigate the catalytic activity of $\text{Ru}(\text{acac})_3$ in dehydrogenation of dimethylamine borane along with isolation and characterization of new species formed during the following reaction.



CHAPTER 2

EXPERIMENTAL

2.1. Materials

Ruthenium(III) acetylacetonate, borane dimethylamine complex (97%), toluene (99.7%) and hexane (99%) were purchased from Aldrich®. Dichloromethane (99%) was purchased from Merck®. All glassware and Teflon coated magnetic stir bars were cleaned and rinsed with acetone before drying at 110 °C for a few hours.

2.2. Equipment

All reactions were carried out under argon or nitrogen atmospheres and conducted in a Parr-5101 low pressure stirred reactor which is connected to a circulating water-bath in order to control temperature (Figure 2.1). Data obtained from the Parr-5101 low-pressure stirred reactor was transmitted to a computer by means of RS-232 module. Hydrogen evolution versus time was recorded by the program called Calgrafix. The temperature was also followed via a thermocouple placed inside the reactor.

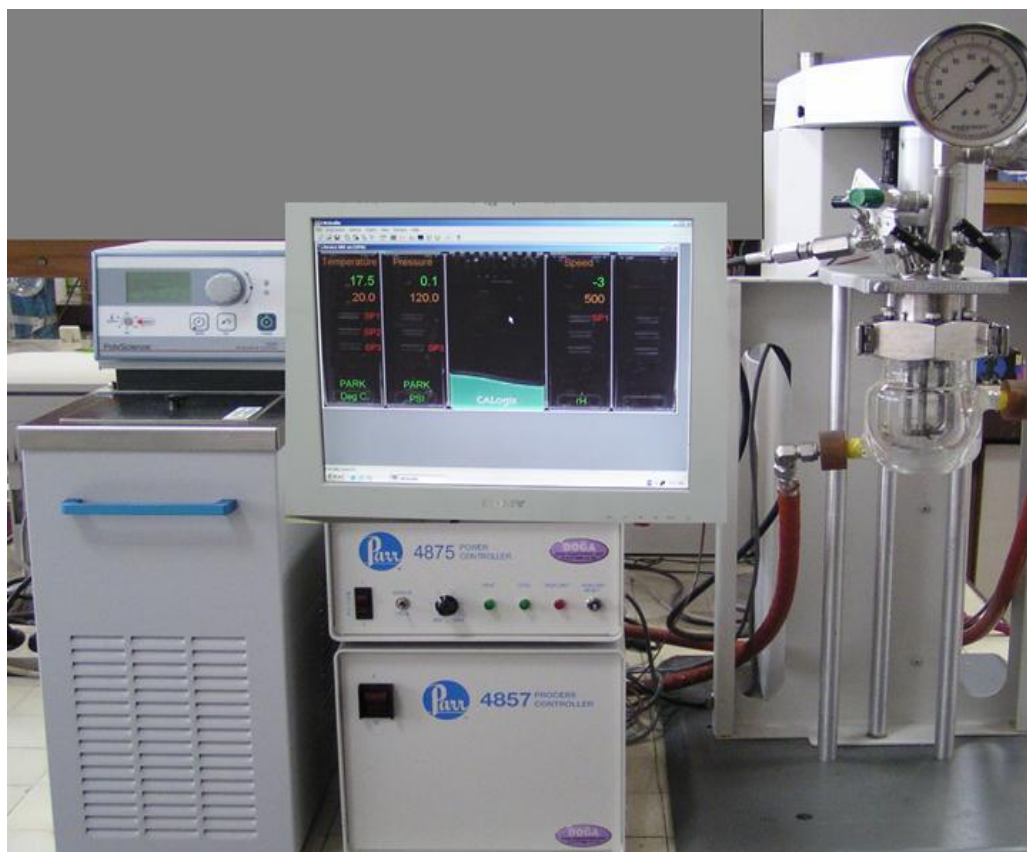


Figure 2.1 The Parr 5101 Low Pressure Stirred Reactor used in catalytic dehydrogenation of dimethylamine borane and measuring the generation of hydrogen from the reaction

^1H NMR and ^{11}B NMR spectra were taken on Bruker Avance DPX 400 MHz spectrometer (400.1 MHz for ^1H -NMR and 128.2 MHz for ^{11}B -NMR). ^1H -NMR chemical shifts are given in ppm (δ) relative to Me_4Si as an internal standard and ^{11}B -NMR chemical shifts are given in ppm (δ) relative to $\text{BF}_3(\text{C}_2\text{H}_5)_2\text{O}$. UV-visible electronic absorption spectra were taken by Shimadzu-2450 double beam spectrometer. The infrared spectrum was recorded from a Vertex 70 ATR/ FTIR spectrometer. Positive ion mass spectrometry data was acquired from a Micro TOF-LC/ESI/Ms system.

2.3. Catalytic dehydrogenation of dimethylamine borane by using ruthenium(III) acetylacetonate

In order to test the catalytic activity of ruthenium(III) acetylacetonate in the dehydrogenation of dimethylamine borane, 294.6 mg (500 mM) dimethylamine borane was dissolved in 10 mL toluene in a reactor thermostated to 60 °C under inert atmosphere. Afterwards, 19.92 mg (5 mM) Ru(acac)₃ was added into the reaction solution. After the addition of Ru(acac)₃, the reactor was closed immediately and stirring at 1000 rpm was tuned on. Hydrogen started to evolve from the reaction and increase pressure inside the reactor. Pressure inside the reactor was recorded in every 5 seconds. The pressure versus time data obtained was converted to the volume of hydrogen evolved versus time by using Microsoft Office Excel 2003.

In order to study the kinetics of dehydrogenation of dimethylamine borane catalyzed by Ru(acac)₃ as a pre-catalyst, all reactions were performed in 10 mL of toluene in which dimethylamine borane (within the range of 200-1000 mM) and Ru(acac)₃ (within the range of 2.5-5.0mM) are dissolved.

Kinetics of dehydrogenation of dimethylamine borane catalyzed by Ru(acac)₃ as a pre-catalyst was investigated depending on substrate concentration, catalyst concentration and temperature. In a series of experiments, NH(CH₃)₂BH₃ concentration was held constant at 500 mM while Ru(acac)₃ concentration was varied within the range of 2.5, 5.0, 7.5 and 10 mM at 60 ± 0.1 °C. In the other set of experiments, Ru(acac)₃ concentration was held constant at 5 mM, while NH(CH₃)₂BH₃

concentration was varied within the range of 200, 400, 500, 600, 800 and 1000 mM at 60 ± 0.1 °C. The third set of experiments were carried out by keeping $\text{NH}(\text{CH}_3)_2\text{BH}_3$ and $\text{Ru}(\text{acac})_3$ concentrations constant at 500 and 5 mM, respectively, and varying the temperature within the range of 50, 55, 60, 65 and 70 °C in order to obtain the activation parameters. In all set of experiments explained above, the hydrogen evolved from the dehydrogenation reaction was monitored and the increase in the pressure of hydrogen gas was recorded by Calgrafix. The pressure versus time data was converted to the volume of hydrogen evolved versus time by using Microsoft Office Excel 2003 and Origin 7.0.

2.4. Catalytic lifetime of ruthenium(III) acetylacetonate pre-catalyst

The catalytic lifetime of $\text{Ru}(\text{acac})_3$ in dehydrogenation of dimethylamine borane was determined by calculating the total turnover number (TTO). Life time experiment was started with 10 mL toluene solution containing 5 mM $\text{Ru}(\text{acac})_3$ and 3000 mM $\text{NH}(\text{CH}_3)_2\text{BH}_3$. Hydrogen gas started to evolve from the reaction. When 75 percent of hydrogen generation was achieved, more $\text{NH}(\text{CH}_3)_2\text{BH}_3$ was added to the reaction solution. By this way, the addition of $\text{NH}(\text{CH}_3)_2\text{BH}_3$ was repeated until no more hydrogen gas was evolved. TTO that is the number of moles of hydrogen evolved per number of moles of ruthenium was calculated.

2.5. Poisoning experiment

In order to understand whether dehydrogenation of dimethylamine borane catalyzed by $\text{Ru}(\text{acac})_3$ is homogenous or heterogeneous, mercury poisoning experiment was carried out [43]. After the 50 % conversion of

reaction was attained, 50 equivalent of mercury per ruthenium was added to the reaction solution including 5 mM Ru(acac)₃ and 500 mM NH(CH₃)₂BH₃.

2.6. Isolation and characterization of in-situ ruthenium(II) species, [Ru{N₂Me₄}₃(acac)H]

19.92 mg Ru(acac)₃ (5 mM) was added into the reaction flask containing 294.6 mg NH(CH₃)₂BH₃ (500 mM) dissolved in 10 mL toluene and thermostated at 60 ± 0.1 °C. Although the complete conversion took 1 hour, the reaction was carried on for 3 h under inert atmosphere and followed by characterization via UV-Vis spectroscopy. After 2 h stirring, the solvent was evaporated in vacuum and the residue was dissolved in the mixture of hexane – dichloromethane. Then, the mixture was put in a fridge in order to precipitate out NH(CH₃)₂BH₃ and the cyclic product formed during dehydrogenation of NH(CH₃)₂BH₃. As a next step, the solution was filtered and evaporated in vacuum giving about 8 mg [Ru{N₂Me₄}₃(acac)H] complex (35 % yield). [Ru{N₂Me₄}₃(acac)H] : ¹H NMR (CDCl₃, ppm): δ -5.60 (br s, 1H, Ru-H), 0.89 (br s, 3H, CH₃), 1.18 (s, 3H, CH₃), 3.42 (br s, 36H, N-CH₃). FTIR (neat, $\bar{\nu}$, cm⁻¹): 2972 m, 2926 m, 1515 m, 1350 – 1470 s, 1020 – 1200 m. UV: λ_{\max} (Toluene, nm) 270. Mass: m/z 463 (M⁺, 100%), 419 (32), 364 (15).

CHAPTER 3

RESULTS AND DISCUSSION

3.1. Catalytic dehydrogenation of dimethylamine borane starting with ruthenium(III) acetylacetonate

Ruthenium(III) acetylacetonate has been found to act as homogeneous catalyst at room temperature in the hydrolysis of sodium borohydride [43]. Moreover, catalytic activity of ruthenium(III) acetylacetonate has been found to be highly enhanced in the presence of different phosphorus compounds [44]. The observation that ruthenium(III) acetylacetonate acts as an effective homogeneous catalyst in the hydrolysis of sodium borohydride prompted us to test its catalytic activity in dehydrogenation of dimethylamine borane in accordance with the following equation:



The conversion of dimethylamine borane to cyclic amine borane appeared to be quantitative as indicated by ^{11}B NMR spectrum of the reaction mixture shown in Figure 3.1. The starting material ($\delta = -13.5$ ppm, quartet) was completely converted to the cyclic amine borane ($\delta = 5.5$ ppm, triplet).

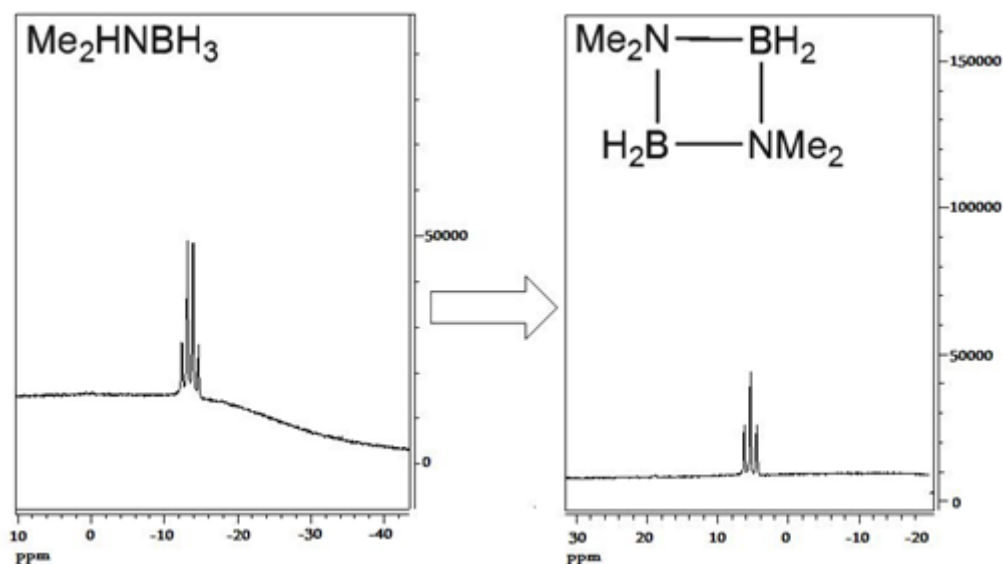


Figure 3.1 ^{11}B NMR spectra of the reaction medium before and after the reaction at $60\text{ }^\circ\text{C}$ ($[\text{DMAB}] = 500\text{ mM}$ and $[\text{Ru}] = 5\text{ mM}$).

The catalytic activity of ruthenium(III) acetylacetonate in the dehydrogenation of dimethylamine borane was tested at room temperature and no catalytic activity was observed. Therefore, the reaction was tested at temperatures in the range $25\text{--}80\text{ }^\circ\text{C}$. Figure 3.2 shows the plots of hydrogen generation versus time during the dehydrogenation of dimethylamine borane (500 mM) starting with ruthenium(III) acetylacetonate (5 mM Ru) in toluene (10 mL) at various temperature. At $25\text{ }^\circ\text{C}$, no hydrogen generation is observed, indicating that ruthenium(III) acetylacetonate does not catalyze the dehydrogenation at room temperature. As the temperature increases, the dehydrogenation of dimethylamine borane takes place at an increasing rate. Thus, the complete reaction is achieved in 6 h at $40\text{ }^\circ\text{C}$, 1 h at $60\text{ }^\circ\text{C}$ and 6 min at $80\text{ }^\circ\text{C}$. Since the dehydrogenation of dimethylamine borane occurs at $60\text{ }^\circ\text{C}$ at a rate suitable to follow the reactions, all the experiments for the kinetic

investigation of the dehydrogenation of dimethylamine borane were carried out at 60 °C.

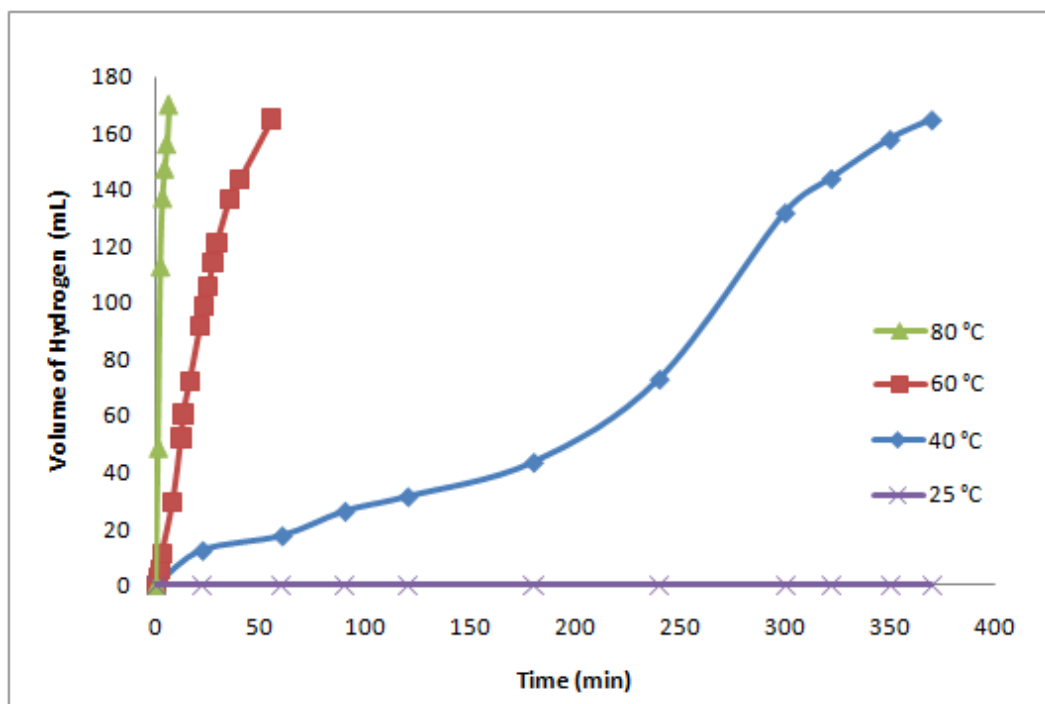


Figure 3.2 Plots of hydrogen volume versus time for the dehydrogenation of dimethylamine borane (500 mM) catalyzed by Ru(acac)₃ (5mM) as pre-catalyst at different temperatures.

It is noteworthy to inspect the hydrogen volume versus time plot for the dehydrogenation of dimethylamine borane at 60 °C in details as given in Figure 3.3. At 60 °C, a slow hydrogen evolution starts immediately. After a certain period of time called induction time, there is an increase in the hydrogen generation rate indicating the formation of a new ruthenium species which has higher catalytic activity in comparison with Ru(acac)₃ as shown in Figure 3.3. The dehydrogenation continues almost linearly until all the dimethylamine borane will be consumed.

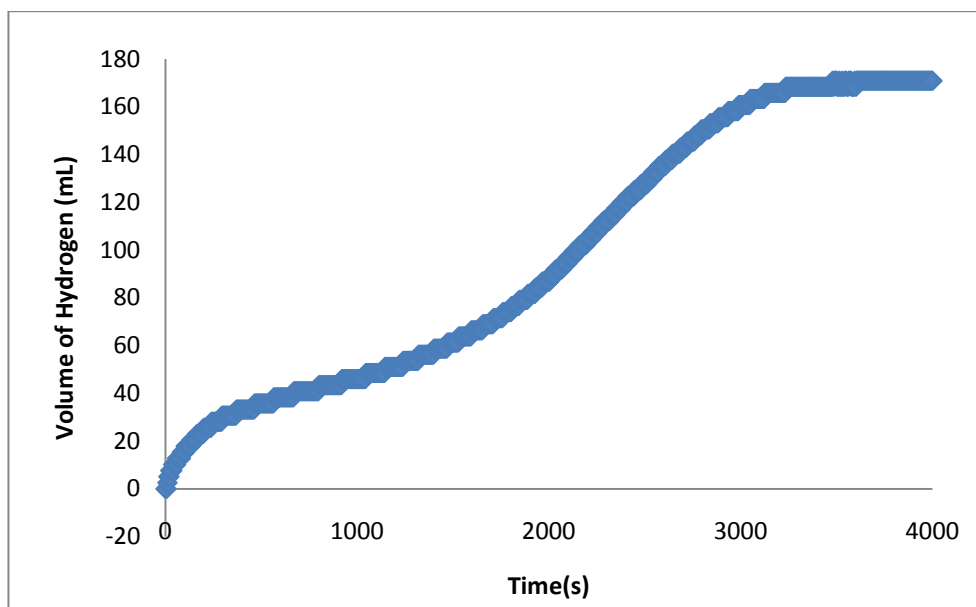


Figure 3.3 Plots of hydrogen volume versus time for the dehydrogenation of dimethylamine borane (500 mM) catalyzed by $\text{Ru}(\text{acac})_3$ (5 mM) as pre-catalyst in 10 mL toluene at 60 °C.

3.2. UV-Visible Spectra

During the induction, the reaction solution gradually changes its color from red to reddish brown, reflecting the reduction of Ru^{3+} . This color change implies that monitoring the UV-vis electronic absorption spectra of the solution may provide a convenient way to follow the conversion. Figure 3.4 shows the UV-vis electronic absorption spectra taken from the solution during the dehydrogenation reaction of dimethylamine borane started with ruthenium(III) acetylacetonate at 60 °C. The UV-visible spectrum of sole $\text{Ru}(\text{acac})_3$ at the beginning of the catalytic reaction exhibits three prominent absorption bands at 270, 350 and 510 nm shown in Figure 3.4. The band at 510 nm is due to the d-d transition while the bands at 270 and 350 nm are attributed to the charge transfer transitions [45]. For a better appreciation of the change in the ruthenium complex, the

catalytic dehydrogenation of dimethylamine borane starting with ruthenium(III) acetylacetonate was followed by UV-Vis spectroscopy for 3 h even though the reaction is complete in 1 h.

As observed in Figure 3.4, the UV-visible spectrum of new ruthenium species (active catalyst) contains an absorption band at 282 nm while the bands of ruthenium(III) acetylacetonate at 350 and 510 nm lose intensity. With regard to similarity of UV-Visible spectrum of the active catalyst with those of octahedral complexes of ruthenium(II), $[\text{Ru}(\text{en})_2\text{IP}]^{2+}$, $[\text{Ru}(\text{en})\text{Phen}]^{2+}$, (IP: imidazo[4,5-*f*][1,10]phenanthroline and phen: 1,10-phenanthroline) [46] and $\text{cis-}[\text{Ru}(\text{acac})_2\{\text{P}(\text{OMe})_3\}_2]$ [47], ruthenium(III) acetylacetonate is likely to be reduced to a ruthenium(II) species in the presence of dimethylamine borane. As seen in figure 3.4, it is noticed that intensity of the absorption bands of ruthenium(III) acetylacetonate decreases while the shoulder at 282 nm grows in. It is noteworthy that the absorption bands of ruthenium(III) acetylacetonate at 270, 350 and 510 nm do not disappear completely even after 3 h. That is, some ruthenium(III) acetylacetonate remains unreacted in the reaction solution.

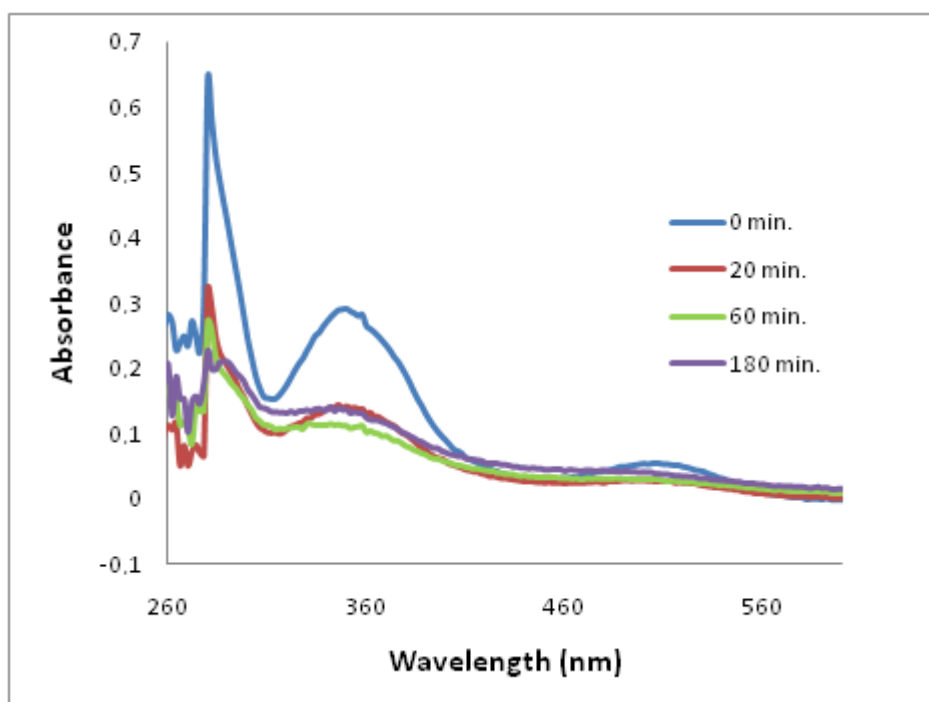


Figure 3.4 UV-visible electronic absorption spectra recorded during the catalytic dehydrogenation of dimethylamine borane starting with $\text{Ru}(\text{acac})_3$.

3.3. Isolation of the ruthenium(II) species

Observation of the reduction of ruthenium(III) to ruthenium(II) inspire us to isolate and characterize the new in-situ formed ruthenium(II) species by FTIR, Mass and ^1H -NMR spectroscopy. When the dehydrogenation of dimethylamine borane in toluene solution was completed (about 3h), toluene was evaporated in vacuum. The residue was dissolved in the mixture of hexane – dichloromethane and then the mixture was placed in a fridge in order to precipitate out the cyclic product formed during dehydrogenation of dimethylamine borane. Afterwards, the solution was filtered and evaporated in vacuum yielding the $[\text{Ru}\{\text{N}_2\text{Me}_4\}_3(\text{acac})\text{H}]$ complex.

3.3.1. Infrared Spectrum

The FTIR spectrum of the isolated ruthenium(II) species shown (Figure 3.5) shows absorption bands characteristic for C-H, N-N and C-N stretchings at 2926 – 2972, 1515 and 1020 – 1200 cm^{-1} , respectively.

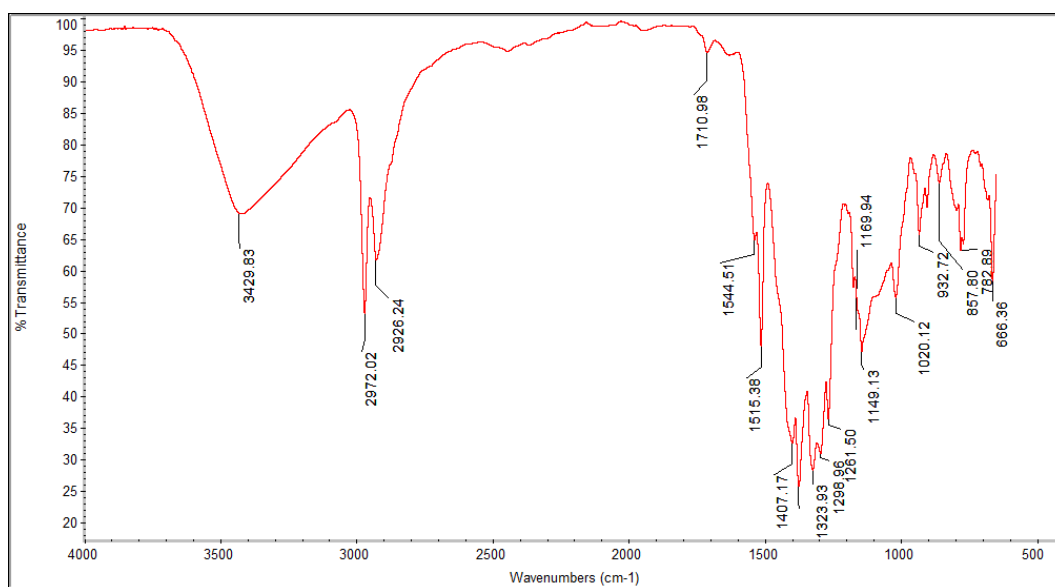


Figure 3.5 FTIR spectrum of the isolated ruthenium(II) species after catalytic dehydrogenation of dimethylamine borane (500mM) starting with $\text{Ru}(\text{acac})_3$ (5mM), taken from the ATR unit.

3.3.2. Mass Spectrum

Mass spectrum of isolated ruthenium(II) species after the reaction shows $[\text{M} - \text{H}]^+$ fragment at $m/z = 463$ as the base peak where $[\text{M}]$ is $[\text{Ru}\{\text{N}_2\text{Me}_4\}_3(\text{acac})\text{H}]$ as seen in Figure 3.6. In addition, two other peaks at $m/z = 419$ and $m/z = 364$ for the $[\text{M} - \text{NMe}_2]^+$ and $[\text{M} - (\text{acac})]^+$ fragments were observed, respectively.

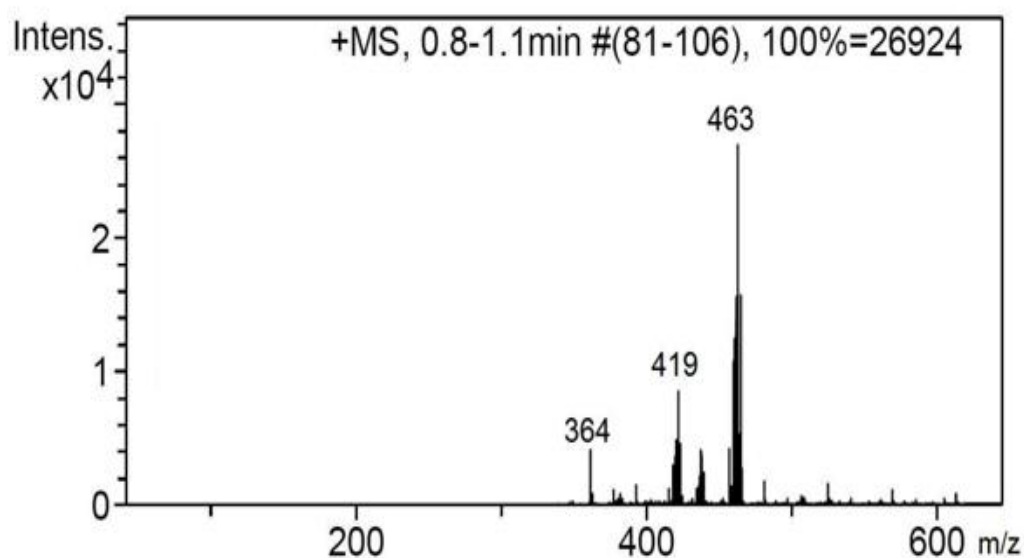


Figure 3.6 Mass spectrum of the ruthenium species, $[\text{Ru}\{\text{N}_2\text{Me}_4\}_3(\text{acac})\text{H}]$, isolated after catalytic dehydrogenation of dimethylamine borane starting with $\text{Ru}(\text{acac})_3$.

3.3.3. ¹H-NMR Spectrum

The ¹H NMR spectrum shown in Figure 3.7, taken from chloroform-d solution, gives a singlet at -5.60 ppm for the hydrogen which is directly coordinated to ruthenium. Two other singlets at 1.18 and 0.89 ppm are attributed to the methyl groups of acetylacetonate. A singlet peak is observed at 3.42 ppm for N – Me groups.

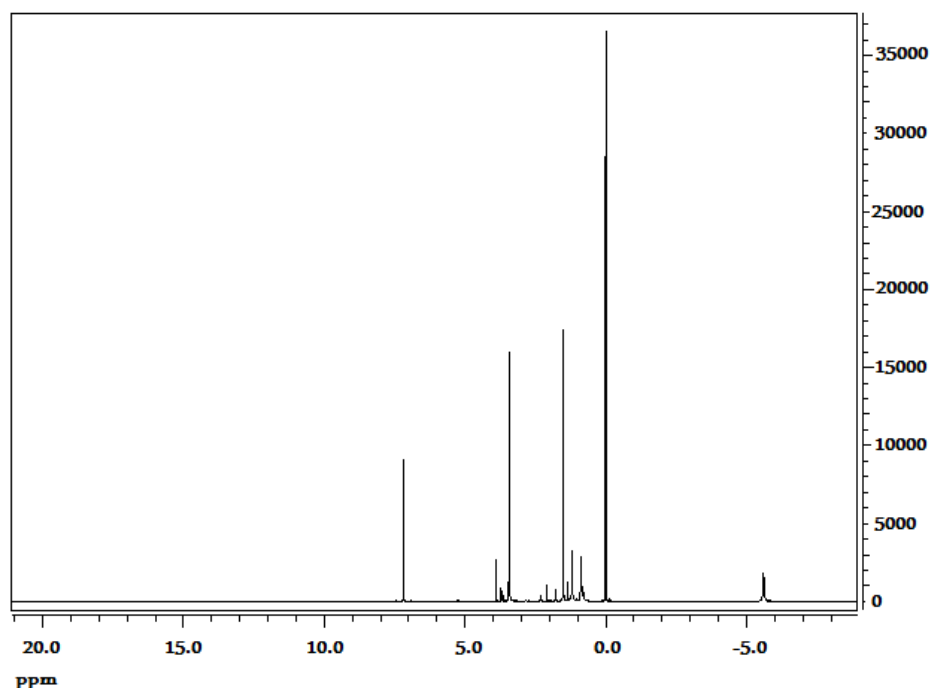


Figure 3.7 ^1H NMR spectrum of the ruthenium species, $[\text{Ru}\{\text{N}_2\text{Me}_4\}_3(\text{acac})\text{H}]$, isolated after catalytic dehydrogenation of dimethylamine borane (500 mM) starting with $\text{Ru}(\text{acac})_3$ (5mM). The peaks at 7 and 1.5 ppm belong to chloroform.

3.3.4 The in-situ formation of ruthenium(II) species, $[\text{Ru}\{\text{N}_2\text{Me}_4\}_3(\text{acac})\text{H}]$, during the catalytic dehydrogenation of dimethylamine borane starting with $\text{Ru}(\text{acac})_3$.

Taking all the results of FTIR, Mass and ^1H -NMR spectroscopy, we envisaged that the isolated ruthenium(II) species may be the octahedral $[\text{Ru}\{\text{N}_2\text{Me}_4\}_3(\text{acac})\text{H}]$ complex (Figure 3.8) which has mer-arrangement of three monodentate N-ligands. Due to the observation of two different peaks in ^1H -NMR spectrum for methyl groups of the acetylacetonato ligand, the octahedral $[\text{Ru}\{\text{N}_2\text{Me}_4\}_3(\text{acac})\text{H}]$ complex is predicted to have meridional arrangement of three N-ligands. The facial-isomer would have

a symmetry plane dividing the acetylacetonato ligand into two equivalent parts.

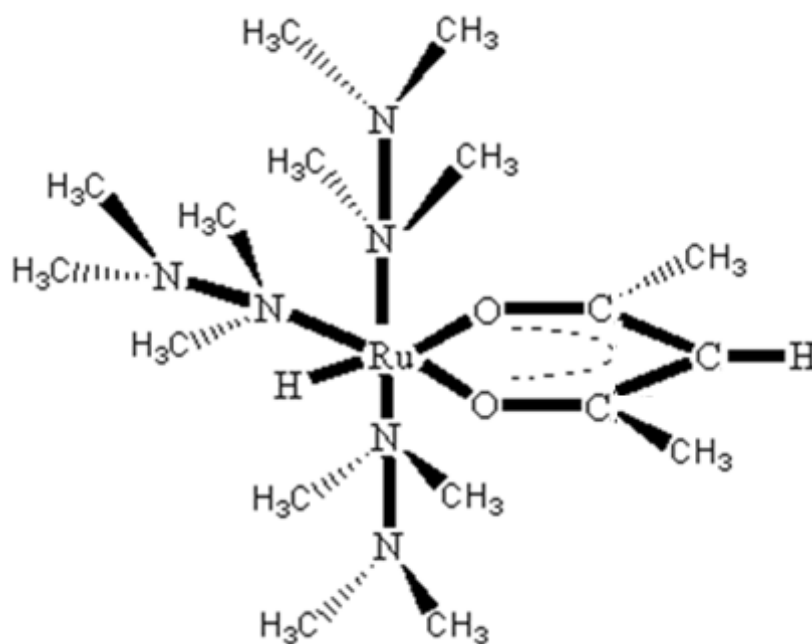
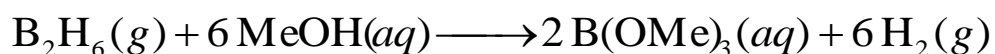


Figure 3.8 A new in situ ruthenium(II) species, $[\text{Ru}\{\text{N}_2\text{Me}_4\}_3(\text{acac})\text{H}]$.

Concerning the formation of $[\text{Ru}\{\text{N}_2\text{Me}_4\}_3(\text{acac})\text{H}]$ complex during the catalytic dehydrogenation of dimethylamine borane starting with ruthenium(III) acetylacetonate, it is likely that dimethylamine borane acts not only as a substrate to produce hydrogen but also as a tetramethyl hydrazine supplier. In addition to the generation of tetramethyl hydrazine from $\text{NH}(\text{CH}_3)_2\text{BH}_3$, gaseous diborane (B_2H_6) is also formed, which can be trapped in the form of trimethylborate by purging the gas into methanol according to the following equation:



Formation of trimethoxy borate is confirmed by ^{11}B NMR spectrum of the methanol solution which shows a peak at 16.37 ppm.

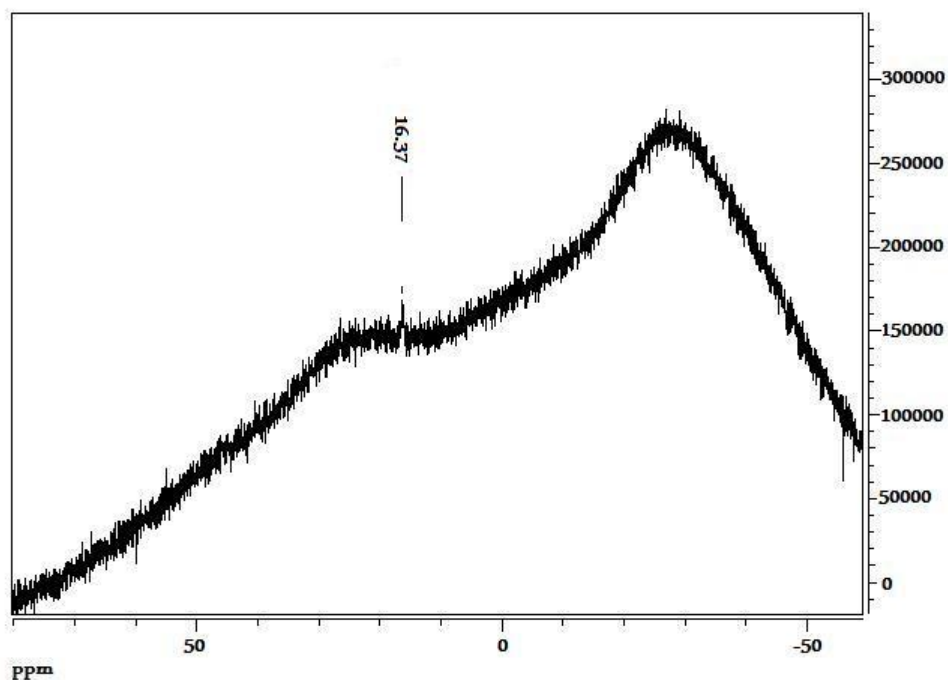


Figure 3.9 ^{11}B NMR spectrum of $\text{B}(\text{OMe})_3$ in methanol trap.

3.4. Poisoning Experiments

A mercury poisoning experiment was performed in order to understand whether the catalytic dehydrogenation of dimethylamine borane starting with ruthenium(III) acetylacetonate is homogeneous or heterogeneous [48]. The hydrogen generation rate in the system comprising ruthenium(III) acetylacetonate pre-catalyst and in-situ formed active catalyst was not affected by the addition of 50 equivalent of mercury to the reaction solution after 50 % conversion of dimethylamine borane. This observation indicates unequivocally that the catalytic reaction is homogeneous.

3.3. Activity of Isolated Ruthenium Species, $[\text{Ru}\{\text{N}_2\text{Me}_4\}_3(\text{acac})\text{H}]$

Isolation of the $[\text{Ru}\{\text{N}_2\text{Me}_4\}_3(\text{acac})\text{H}]$ complex was achieved in 35 % yield. Isolated ruthenium species, $[\text{Ru}\{\text{N}_2\text{Me}_4\}_3(\text{acac})\text{H}]$, was employed as a homogeneous catalyst in dehydrogenation of dimethylamine borane which shows a catalytic activity in hydrogen evolution comparable with the second linear portions of volume of hydrogen vs. time plot for the reaction starting with ruthenium(III) acetylacetonate.

In order to compare the hydrogen evolution in dehydrogenation of dimethylamine borane starting with $\text{Ru}(\text{acac})_3$ and $[\text{Ru}\{\text{N}_2\text{Me}_4\}_3(\text{acac})\text{H}]$, respectively, the data belonging to $[\text{Ru}\{\text{N}_2\text{Me}_4\}_3(\text{acac})\text{H}]$ was corrected by a factor of 3 in Figure 3.10. On the contrary to ruthenium(III) acetylacetonate when the $[\text{Ru}\{\text{N}_2\text{Me}_4\}_3(\text{acac})\text{H}]$ complex is employed as catalyst in the dehydrogenation of dimethylamine borane, hydrogen generation starts immediately without induction time since a preformed catalyst is used in the catalytic reaction.

This observation indicates that the $[\text{Ru}\{\text{N}_2\text{Me}_4\}_3(\text{acac})\text{H}]$ complex is acting as a catalyst in the dehydrogenation of dimethylamine borane. However, it remains unclear whether this ruthenium(II) species is the active catalyst or a conversion product of the active catalyst.

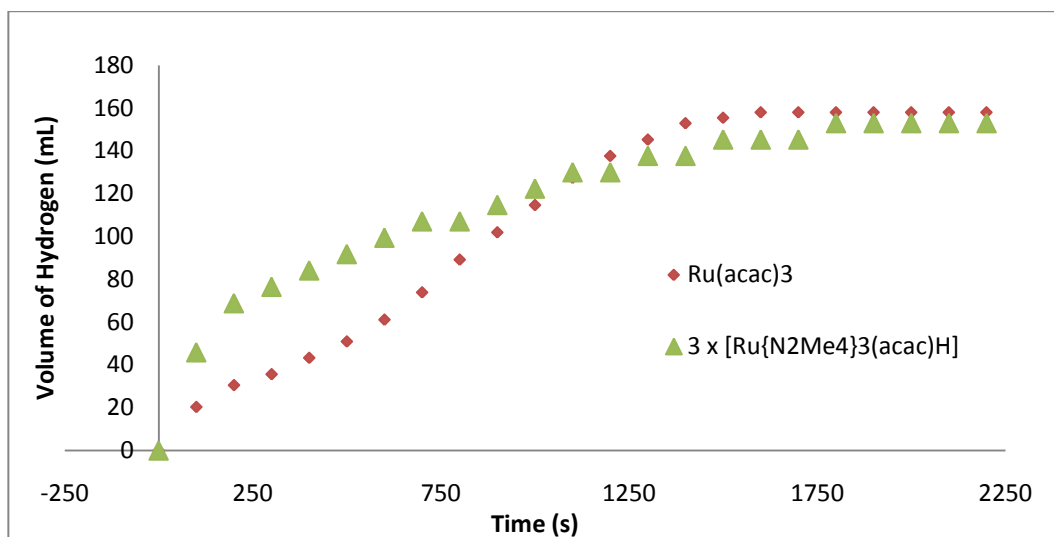


Figure 3.10 Comparison of dehydrogenation of dimethylamine borane (500 mM) catalyzed by Ru(acac)₃ (5 mM) and isolated ruthenium species, [Ru{N₂Me₄}₃(acac)H] (1.65 mM) at 60.0 ± 0.1 °C. The data obtained for the latter complex was corrected by a factor of 3.

3.4. Kinetic Study

Kinetics of the dehydrogenation of dimethylamine borane in the presence of ruthenium(III) acetylacetonate was studied by monitoring hydrogen generation depending on catalyst concentration, substrate concentration and temperature. Figure 3.11 shows the volume of hydrogen versus time plots during dehydrogenation of dimethylamine borane solution (500 mM) starting with ruthenium(III) acetylacetonate in different ruthenium concentrations at 60.0 ± 0.1 °C.

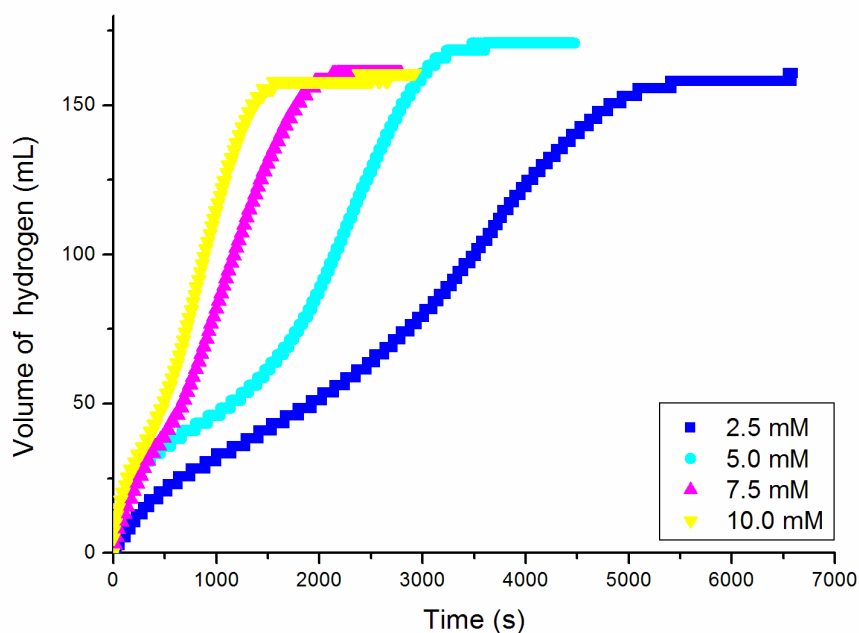


Figure 3.11 Plots of hydrogen volume versus time for the dehydrogenation of dimethylamine borane (500 mM) catalyzed by $\text{Ru}(\text{acac})_3$ as pre-catalyst with different ruthenium concentrations at 60 °C.

The inspection of the plots in Figure 3.11 reveals the following points: (i) The increasing catalytic activity observed after a certain period of time (induction time) in each case is indicative of the formation of active species from the reaction of ruthenium(III) acetylacetonate and dimethylamine borane during the induction time. (ii) The active species has higher catalytic activity in comparison to the initial activity of ruthenium(III) acetylacetonate which acts as a pre-catalyst. (iii) The induction time for the formation of active catalyst decreases with the increasing concentration of ruthenium(III) acetylacetonate. (iv) On the contrary to this, the catalytic activity during the induction time increases with the increasing concentration of ruthenium(III) acetylacetonate. (v) After

induction period, an almost linear hydrogen evolution continues until all the dimethylamine borane will be consumed.

The rate of hydrogen generation was determined from the slope of the linear portion of plots after the induction time. The hydrogen generation rate increases with the increasing concentration of ruthenium(III) acetylacetonate. In order to calculate the reaction order with respect to catalyst concentration, hydrogen generation rate vs. catalyst concentration both in logarithmic scales was plotted which gives a straight line (Figure 3.12). The slope of this line is $1.025 \approx 1.0$ indicating that the hydrogen evolution from the dehydrogenation of dimethylamine borane is first-order with respect to the ruthenium concentration.

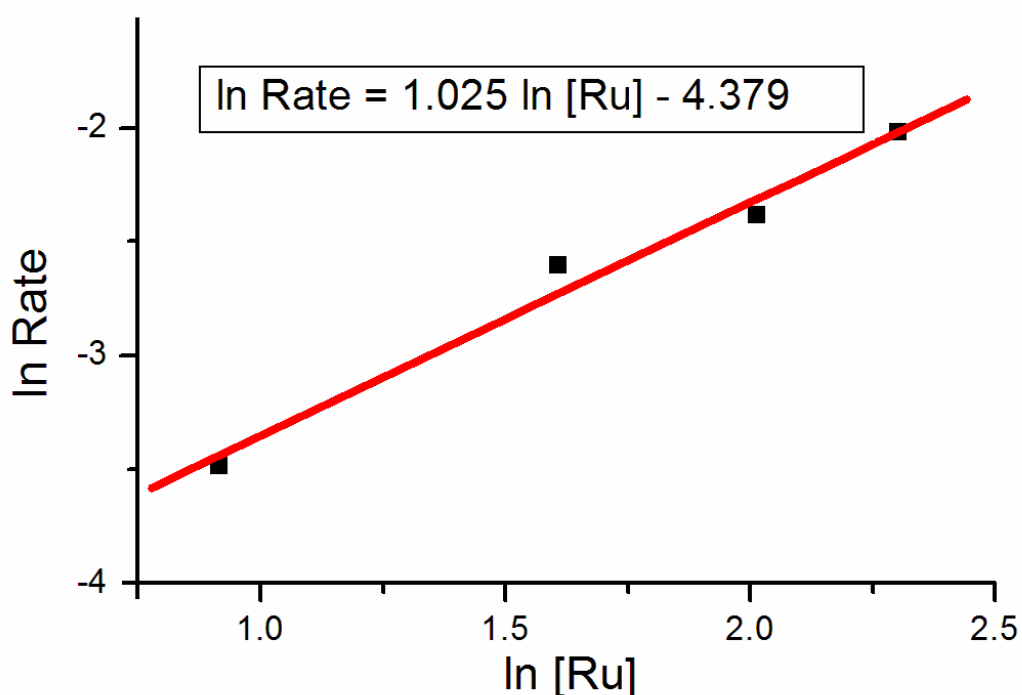


Figure 3.12 Plot of hydrogen generation rate versus the concentration of ruthenium (both in logarithmic scales) for the dehydrogenation of dimethylamine borane (500 mM) started with $\text{Ru}(\text{acac})_3$ at $60\text{ }^\circ\text{C}$ after the induction time.

The effect of substrate concentration on the hydrogen evolution rate was determined by varying the concentration of $\text{NH}(\text{CH}_3)_2\text{BH}_3$ at a constant ruthenium concentration of 5.0 mM and temperature of 60 ± 0.1 °C. (Figure 3.13)

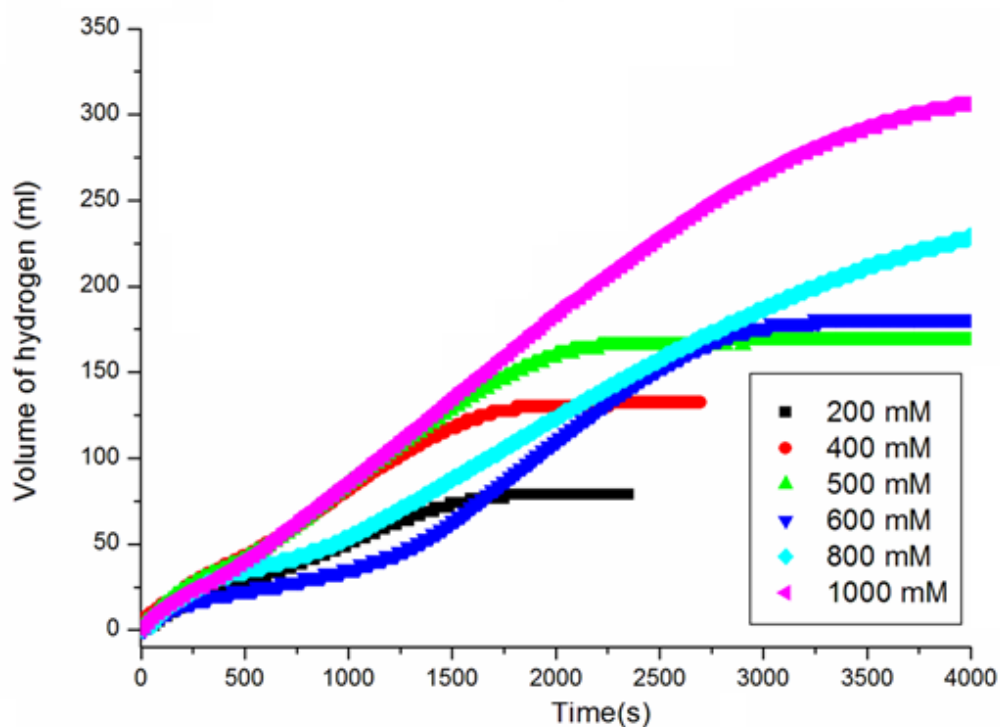


Figure 3.13 Plots of hydrogen volume versus time for the dehydrogenation of dimethylamine borane catalyzed by 5 mM $\text{Ru}(\text{acac})_3$ as pre-catalyst with different substrate concentrations at 60 °C.

The rate of hydrogen generation was determined from the slope of the linear portion of plots after the induction time. The hydrogen evolution rate does not show a significant variation with the increasing concentration of dimethylamine borane. In order to calculate the reaction order with respect to dimethylamine borane concentration, hydrogen generation rate vs. dimethylamine borane concentration, both in

logarithmic scales was plotted (Figure 3.14). The plot of hydrogen generation rate versus $\text{NH}(\text{CH}_3)_2\text{BH}_3$ concentration in logarithmic scale gives a straight line with a slope of about zero. This indicates that the dehydrogenation of dimethylamine borane is zero-order with respect to the substrate concentration, at least in the range of 0.2 – 1.0 M $\text{NH}(\text{CH}_3)_2\text{BH}_3$, in the presence of ruthenium(III) acetylacetonate.

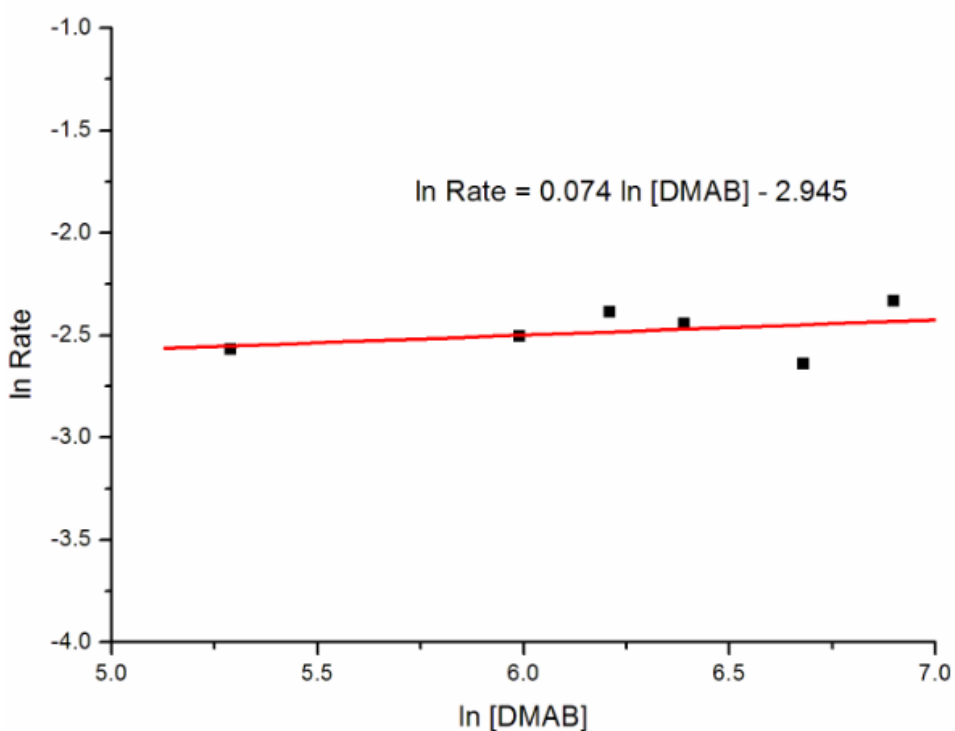


Figure 3.14 Plot of hydrogen generation rate versus the concentration of dimethylamine borane (both in logarithmic scales) for the dehydrogenation of dimethylamine borane started with $\text{Ru}(\text{acac})_3$ (5 mM) at 60 °C after the induction time.

Thus the rate law for the catalytic dehydrogenation of dimethylamine borane can be given as:

$$-\frac{d[\text{NH}(\text{CH}_3)_2\text{BH}_3]}{dt} = \frac{d[\text{H}_2]}{dt} = k[\text{Ru}]$$

Dehydrogenation of dimethylamine borane was carried out at various temperatures in the range of $50\text{-}70 \pm 0.1$ °C starting with a solution containing 500 mM dimethylamine borane and 5.0 mM ruthenium(III) acetylacetonate (Figure 3.15).

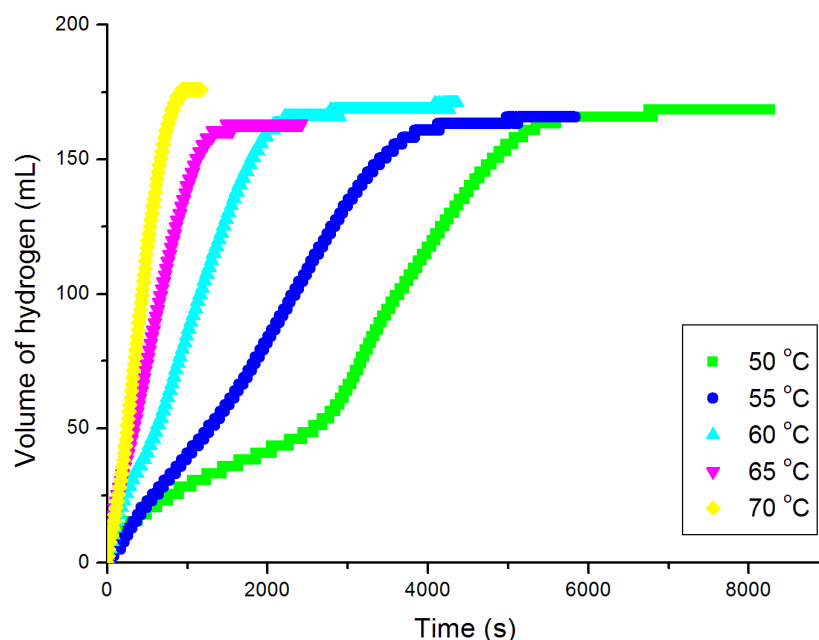


Figure 3.15 Plots of hydrogen volume versus time for dehydrogenation of dimethylamine borane starting with a solution containing 500 mM $\text{NH}(\text{CH}_3)_2\text{BH}_3$ and 5 mM $\text{Ru}(\text{acac})_3$ at various temperatures.

The examination of the plots in Figure 3.15 reveals the following points: (i) The induction time for the formation of active catalyst decreases with the increasing temperature. (ii) The catalytic activity of both the precatalyst ruthenium(III) acetylacetonate and the in situ formed active species

increases with the increasing temperature. (iii) After the induction time, the values of the rate constant k were determined from the linear part of the plots considering the rate dependency on temperature (Table 3.1) in order to attain the activation parameters for the catalytic dehydrogenation of dimethylamine borane by using either Arrhenius or Eyring plot.

Table 3.1 Values of the rate constant k in $(\text{mol H}_2) \cdot (\text{mol Ru})^{-1} \cdot \text{s}^{-1}$ for dehydrogenation of dimethylamine borane (500 mM) catalyzed by ruthenium(III) acetylacetonate (5 mM) at different temperatures.

T(°C)	k ($[\text{mol H}_2] \cdot [\text{mol Ru}]^{-1} \cdot \text{s}^{-1}$)
50	$1.30 \pm 0.07 \times 10^{-5}$
55	$1.72 \pm 0.09 \times 10^{-5}$
60	$2.97 \pm 0.15 \times 10^{-5}$
65	$4.67 \pm 0.23 \times 10^{-5}$
70	$7.95 \pm 0.40 \times 10^{-5}$

For the determination of the activation energy, the rate constant and temperature were evaluated by using following Arrhenius equation:

$$\ln k = \ln A - \left(\frac{E_a}{RT} \right)$$

where E_a is activation energy, R is gas constant and T is temperature.

The Arrhenius activation energy was found to be $85 \pm 2 \text{ kJ.mol}^{-1}$ for the catalytic dehydrogenation of dimethylamine borane starting with ruthenium(III) acetylacetonate.

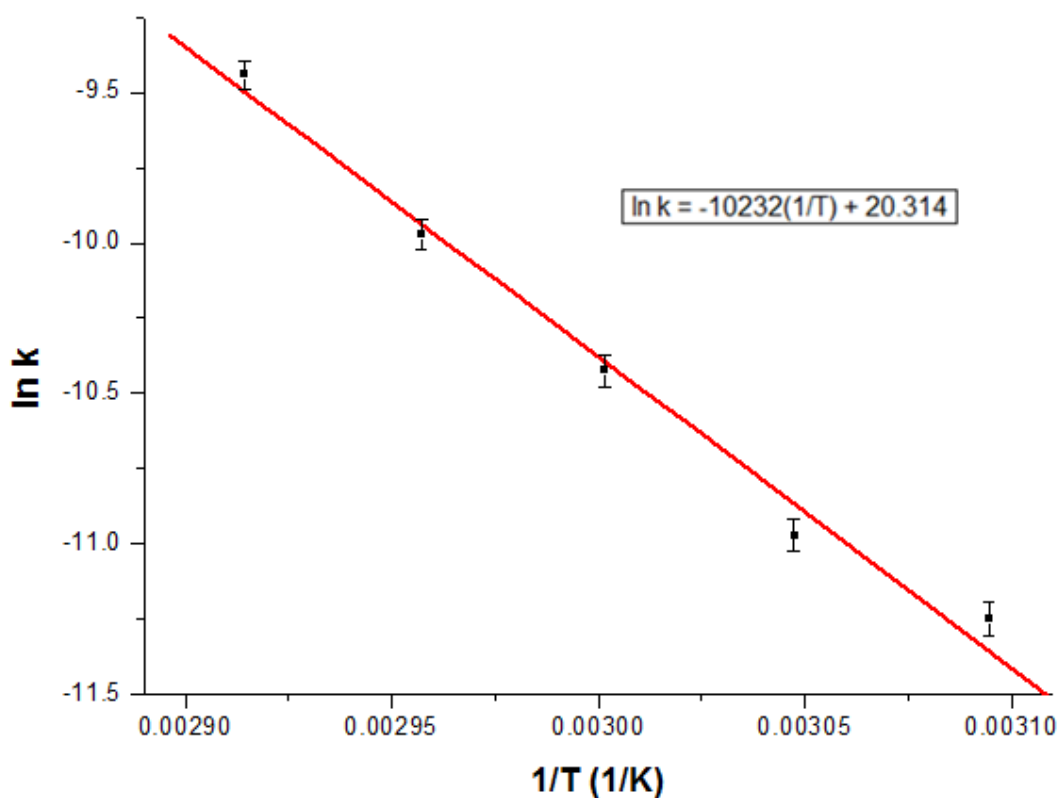


Figure 3.16 Arrhenius plot for dehydrogenation of dimethylamine borane starting with a solution containing 500 mM $\text{NH}(\text{CH}_3)_2\text{BH}_3$ and 5.0 mM $\text{Ru}(\text{acac})_3$ at different temperatures.

In order to calculate the enthalpy of activation and the entropy of activation, Eyring equation was used.

$$\ln \frac{k}{T} = \frac{1}{T} \left(\frac{-\Delta H^*}{R} \right) + \ln \frac{k_b}{h} + \frac{\Delta S^*}{R}$$

where k is rate constant, T is temperature, ΔH^\ddagger is activation enthalpy, ΔS^\ddagger is activation entropy, k_b is Boltzmann constant, h is Planck's constant and R is gas constant.

The evaluation of rate constant versus temperature data by using Eyring equation provides the activation enthalpy and the activation entropy values: $\Delta H^\ddagger = 82 \pm 2 \text{ kJ.mol}^{-1}$ and $\Delta S^\ddagger = -85 \pm 5 \text{ J.mol}^{-1}\text{K}^{-1}$. The large negative value of activation entropy indicates that the mechanism for the catalytic dehydrogenation of dimethylamine borane starting with ruthenium(III) acetylacetonate has an associative nature in the transition state [49,50].

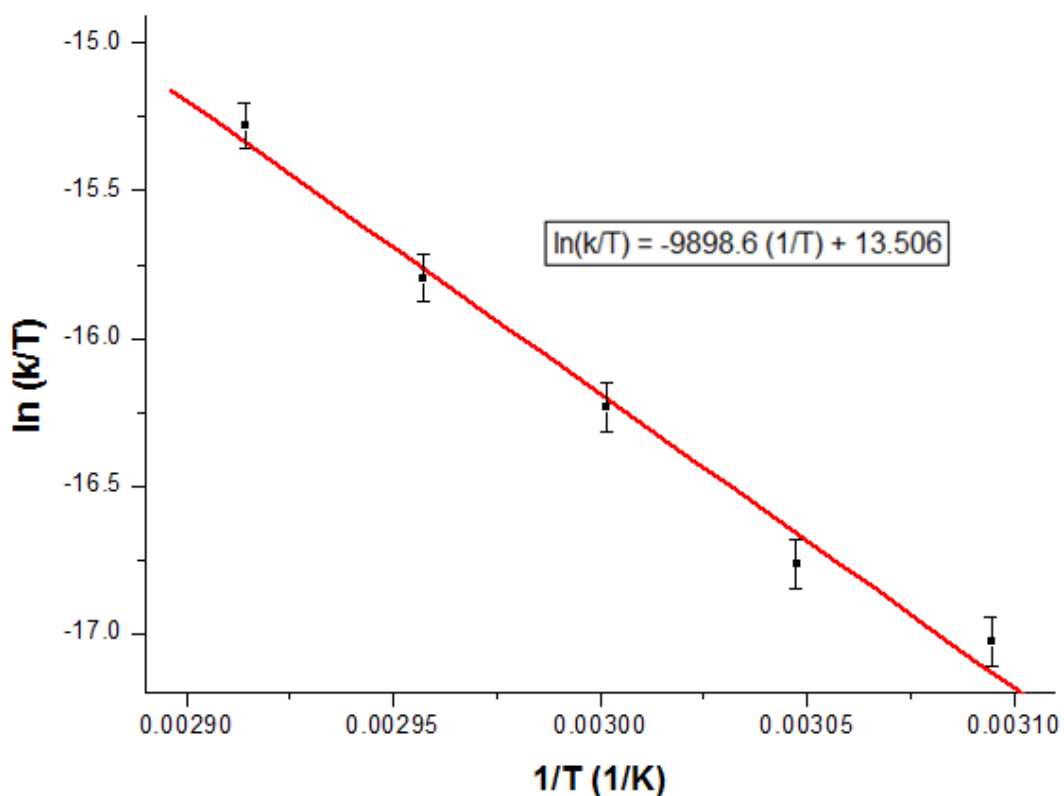


Figure 3.27 Eyring plot for dehydrogenation of dimethylamine borane starting with a solution containing 500 mM $\text{NH}(\text{CH}_3)_2\text{BH}_3$ and 5 mM $\text{Ru}(\text{acac})_3$ at different temperatures.

3.5 The Catalytic Life Time

The system obtained starting with ruthenium(III) acetylacetonate and diethylamine borane appears to be a stable and long-live catalyst in dehydrogenation of dimethylamine borane. Lifetime of the catalyst was measured by determining the total turnover number (TTON) in hydrogen generation from dehydrogenation of dimethylamine borane at 60 ± 0.1 °C. Figure 3.18 shows the variation in the turnover number with time during the dehydrogenation of dimethylamine borane starting with ruthenium(III) acetylacetonate in toluene at 60 ± 0.1 °C.

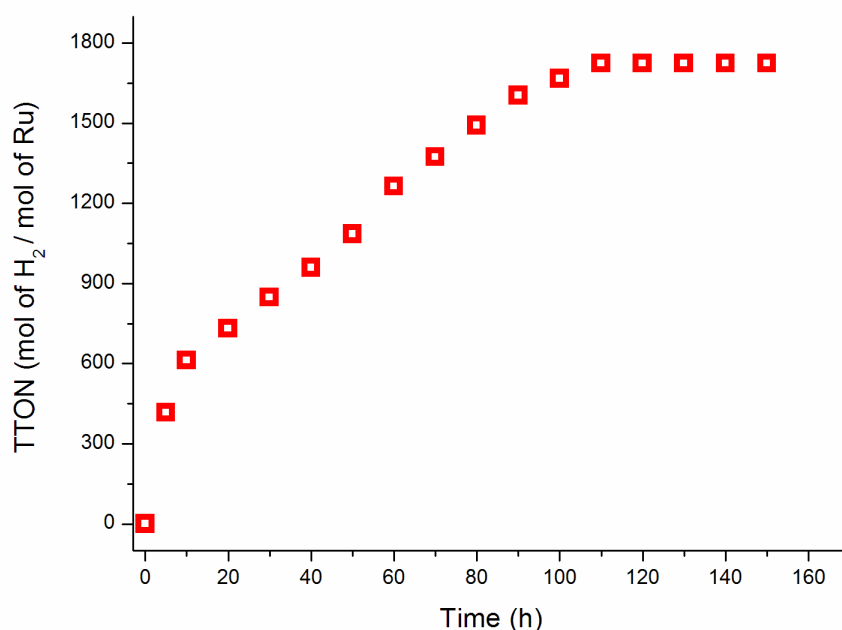


Figure 3.28 Plot of total turnover number versus time for dehydrogenation of dimethylamine borane (3000 mM) starting with ruthenium(III) acetylacetonate (5 mM Ru) in 10 mL toluene at 60 °C.

The catalyst formed from the reduction of ruthenium(III) acetylacetonate provides 1700 turnovers over 100 h in the hydrogen generation from the dehydrogenation of dimethylamine borane in toluene at 60 ± 0.1 °C. The highest value of turnover frequency (TOF) was found to be 37.5 (mol H₂)(mol Ru)⁻¹(h)⁻¹ for the catalytic dehydrogenation of dimethylamine borane in toluene at 60 ± 0.1 °C.

CHAPTER 4

CONCLUSIONS

In summary, our study on ruthenium(III) acetylacetonate catalyst in dehydrogenation of dimethylamine borane leads to the following conclusions and insights, some of which were previously unavailable:

- Ruthenium(III) acetylacetonate is a pre-catalyst in the dehydrogenation of dimethylamine borane, being converted to an active catalyst.
- A new ruthenium species is formed during the catalytic dehydrogenation of dimethylamine borane starting with ruthenium(III) acetylacetonate after the induction time and isolated in the form of *mer*-[Ru{N₂Me₄}₃(acac)H] complex.
- Increasing the concentration of ruthenium(III) acetylacetonate and applying higher temperature lead to a decrease in the induction time and an increase in the formation rate of active catalyst.
- The new ruthenium(II) complex, [Ru{N₂Me₄}₃(acac)H], isolated from the catalytic reaction solution, is found to be more active than ruthenium(III) acetylacetonate in the dehydrogenation of dimethylamine borane.

- Dehydrogenation of dimethylamine borane starting with ruthenium(III) acetylacetonate is first-order with respect to the catalyst concentration and zero-order with respect to substrate concentration.
- The rate law for catalytic dehydrogenation of dimethylamine borane starting with ruthenium(III) acetylacetonate was established to be;

$$-\frac{d[\text{NH}(\text{CH}_3)_2\text{BH}_3]}{dt} = \frac{d[\text{H}_2]}{dt} = k[\text{Ru}]$$

- The catalyst formed from the reduction of ruthenium(III) acetylacetonate provides 1700 turnovers over 100 h in the hydrogen generation from dehydrogenation of dimethylamine borane before it is deactivated. However, whether the isolated $[\text{Ru}\{\text{N}_2\text{Me}_4\}_3(\text{acac})\text{H}]$ complex is the catalytically active species or a conversion product of the active catalyst is still not clear yet.
- The activation parameters of catalytic dehydrogenation of dimethylamine borane starting with ruthenium(III) acetylacetonate were determined from the evaluation of the kinetic data: activation energy; $E_a = 85 \pm 2 \text{ kJmol}^{-1}$, the enthalpy of activation; $\Delta H^\ddagger = 82 \pm 2 \text{ kJmol}^{-1}$ and the entropy of activation; $\Delta S^\ddagger = -85 \pm 5 \text{ Jmol}^{-1}\text{K}^{-1}$.

REFERENCES

- [1] Zerta, M., Schmidt, P.R., Stiller, C., Landinger, H., *Int. J. Hydrogen Energy*, **2008**, 33, 3021.
- [2] Basic Research Needs For the Hydrogen Economy, Report of the Basic Energy Sciences Workshop on Hydrogen Production, Storage and Use, May 13-15, **2003**, Office of Sciences, U.S. Department of Energy, www.sc.doe.gov/bes/hydrogen.pdf.
- [3] Vriessa, B.J.M., Vuuren, D.P., Hoogwijk, M.M., *Energy Policy*, **2007**, 35, 2590.
- [4] Sibley, R., *Our Future Is Hydrogen, Environment, and Economy*, New Science Publications, Wellington, USA, **2001**.
- [5] Schlapbach, L., Züttel, A., *Hydrogen-storage materials for mobile applications*, *Nature*, **2001**, 414, 353.
- [6] Amendola, S.C., Sharp-Goldman, S.L., Saleem Janjua, M., Kelly, M.T., Petillo, P.J., *A safe, portable, hydrogen gas generator: aqueous, alkaline borohydride solutions and Ru catalyst*, *J. Power Sources*, **2000**, 420, 302-4.
- [7] Chen, P., Xiong, Z., Luo, J., Lin, J., Tan, K.L., *Nature*, **2002**, 420, 302.
- [8] Amendola, S.C., Sharp-Goldman, S.L., Janjua Saleem, M., Kelly, M.T., Petillo, P.J., Binder, M., *J. Power Sources*, **2000**, 85, 186.
- [9] Amendola, S.C., Sharp-Goldman, S.L., Janjua Saleem, M., Spencer, N.C., Kelly, M.T., Petillo, P.J., *Int. J. Hydrogen Energy*, **2000**, 25, 969.
- [10] Umegaki, T., Yan, J.M., Zhang, X.B., Shioyama, H., Kuriyama, N., Xu, Q., *Int. J. Hydrogen Energy*, **2009**, 34, 2303.
- [11] Dixon, D.A., Gutowski, M.J., *J. Phys. Chem. A*, **2005**, 109, 5129.
- [12] Nguyen, M.T., Nguyen, V.S., Matus, M.H., Gopakumar, G., Dixon, D.A., *J. Phys. Chem A*, **2007**, 111, 679.

- [13] Fulton, C.Y., Linehan, J.L., Autrey, J.C., *J. Am. Chem. Soc.*, **2005**, 127, 3254.
- [14] Jaska, C.A., Clark, T.J., Clendenning, S.B., Grozea, D., Turak, A., Lu, Z.H., Manners, I., *J. Am. Chem. Soc.*, 127 **2005**, 127, 5116.
- [15] Jaska, C.A., Manners, I., *J. Am. Chem. Soc.*, **2004**, 126, 9776.
- [16] Jaska, C.A., Manners, I., *J. Am. Chem. Soc.*, **2004**, 126, 2698.
- [17] Jaska, C.A., Manners, I., *J. Am. Chem. Soc.*, **2004**, 126, 1334.
- [18] Jaska, C.A., Temple, K., Lough, A.J., Manners, I., *J. Am. Chem. Soc.*, **2003**, 125, 9424.
- [19] Yoon, C.W., Sneddon, L.G., *J. Am. Chem. Soc.*, **2006**, 128, 13992.
- [20] Clark, T.J., Lee, K., Manners, I., *Chem. Eur. J.*, **2006**, 12, 8634.
- [21] Jaska, C.A., Temple, K., Lough, A.J., Manners, I., *Phosphorus, sulfur and silicon*, **2004**, 179, 733.
- [22] Durap, F., Zahmakıran, M., Ozkar, O., *Appl. Catal. A: General*, **2009**, 369, 53.
- [23] Zahmakıran, M., Ozkar, S., *Inorg. Chem.*, **2009**, 48, 8955.
- [24] Zahmakıran, M., Durap, F., Ozkar, S., *Int. J. Hydrogen Energy*, **2010**, 35, 187.
- [25] Metin, O., Sahin, S., Ozkar, S., *Int. J. Hydrogen Energy*, **2009**, 34, 6304.
- [26] Chandra, M., Xu, Q., *Journal of Power Sources*, **2007**, 168, 135.
- [27] Xu, Q., Chandra, M., *Journal of Power Sources*, **2006**, 163, 364.
- [28] Benedetto, S.D., Carewska, M., Cento, C., Gislou, P., Pasquali, M., Scaccia, S., Procini, P.P., *Thermochim. Acta*, **2006**, 441, 184.
- [29] Mohajeri, N., Raissi, A.T., Adebıyi, O., *Journal of Power Sources*, **2007**, 167, 482.
- [30] Cheng, F., Ma, H., Li, Y., Chen, J., *Inorg. Chem.*, **2007**, 46, 788.
- [31] Denney, M.C., Pons, V., Hebden, T.J., Heinekey, D.M., Goldberg, K.I., *J. Am. Chem. Soc.*, **2006**, 128, 12048.

- [32] Clark, T.J, Russell, C.A., Manners, I., *J. Am. Chem. Soc.*, **2006**, 128, 9582.
- [33] Keaton, R.J., Blacquiere, J.M., Baker, R.T., *J. Am. Chem. Soc.*, **2007**, 129, 1844.
- [34] Gutowska, A., Li, L., Shin, Y., Wang, C.M., Li, X.S., Linehan, J.C., Smith, R.S., Kay, B.D., Schmid, B., Shaw, W., Gutowski, M., Autrey, T., *Angew. Chem. Int. Ed.*, **2005**, 44, 3578.
- [35] Chandra, M., Xu, Q., *Journal of Power Sources*, **2006**, 159, 855.
- [36] Stephens, F.H, Baker, R.T., Matus, M.H., Grant, D.J., Dixon, D.A., *Angew. Chem. Int. Ed.*, **2007**, 46, 746.
- [37] Bluhm, M.E., Bradley, M.G., Butterick, R., Kusari, U., Sneddon, L.G., *J. Am. Chem. Soc.*, **2006**, 128, 7748.
- [38] Wang, J.S, Geanangel, R.A., *Inorg. Chim. Acta*, **1988**, 148, 185.
- [39] Wolf, G., Baumann, J., Baitalow, F., Hoffmann, F.P., *Thermochim. Acta*, **2000**, 343, 19.
- [40] Baumann, J., Baitalow, F., Wolf, G., *Thermochim. Acta*, **2005**, 430, 9.
- [41] Jaska, C.A., Temple, K., Lough, A.J., Manners, I., *J. Am. Chem. Soc.*, **2003**, 125, 9424.
- [42] Keceli, E., Ozkar, S., *J. Mol. Catal. A: Chem.*, **2008**, 286, 87.
- [43] Widegren, J.A., Finke, R.G., *J. Mol. Catal. A: Chem.*, **2003**, 198, 317.
- [44] Masjedi, M., Demiralp, T., Ozkar, S., *J. Mol. Catal. A: Chem.*, **2009**, 310, 59.
- [45] Grobelny, R., Jeowska-Trzebiatowska, B., Wojciechowski, W., *J. Inorg. Nucl. Chem.*, **1966**, 28, 2715.
- [46] Nagababu, P., Latha, J.N.L., Satyanarayana, S., *Chem. Biodiversity*, **2006**, 3, 1219.
- [47] Masjedi, M., Yildirim, L.T., Ozkar, S., *Inorg. Chim. Acta*, **2010**, 363, 1713.
- [48] Widegren, J.A., Finke, R.G., *J. Mol. Catal. A: Chem.*, **2003**, 198, 317.

[49] Connors, K.A., *Theory of Chemical Kinetics*, VCH Publishers, New York, **1990**.

[50] Twigg, M.V., *Mechanism of Inorganic and Organometallic Reactions*, Plenum Press, New York, **1994**.